AIAA Meeting Papers on Disc, July 1996
A9636940, F49620-95-1-0331, AIAA Paper 96-2706

RF signal impact study of an SPT

Shawn G. Ohler
Michigan Univ., Ann Arbor

Alranzo B. Ruffin
Michigan Univ., Ann Arbor

Brian E. Gilchrist
Michigan Univ., Ann Arbor

Alec D. Gallimore
Michigan Univ., Ann Arbor

AIAA, ASME, SAE, and ASEE, Joint Propulsion Conference and Exhibit, 32nd, Lake Buena Vista, FL, July 1-3, 1996

Stationary plasma thrusters (SPTs) are currently being tested and considered for use aboard next generation spacecraft for North-South stationkeeping, repositioning, and orbit transfer due to their high thrust efficiency and nearly optimal specific impulse (Isp). However, because the thruster's plume generates plasma densities with corresponding plasma frequencies approaching 3 GHz, consideration must be given to possible interactions with satellite electromagnetic systems (communication, navigation, remote-sensing). The plume potentially can degrade the EM link through attenuation as well as added amplitude or phase noise. We provide the physical mechanism and ray tracing modeling method to understand the possible amplitude modulation produced by the SPT thruster and experimentally quantify the rather significant plume impact to phase and amplitude for a signal at 1.575 GHz (GPS frequency) which is outside the theoretical limit of the modeling technique. (Author)

RF SIGNAL IMPACT STUDY OF AN SPT

Shawn G. Ohler* Alranzo B. Ruffin†,
Brian E. Gilchrist‡, and Alec D. Gallimore§
University of Michigan
Ann Arbor, MI

Abstract

Stationary plasma thrusters (SPT's) are currently being tested and considered for use aboard next generation spacecraft for North-South station keeping, repositioning, and orbit transfer due to their high thrust efficiency and nearly optimal specific impulse (I_{sp}). However, because the thruster's plume generates plasma densities with corresponding plasma frequencies approaching 3 GHz, consideration must be given to possible interactions with satellite electromagetic systems such as for communication, navigation, and remote-sensing. The plume potentially can degrade the electromagnetic link through attenuation as well as added amplitude or phase noise. Previous experimental and theoretical studies have investigated the phase modulation at a range of frequencies and have experimentally verified signal attenuation. This paper provides the physical mechanism and ray tracing modeling method to understand the possible amplitude modulation produced by the SPT thruster. The study also experimentally quantifies the rather significant plume impact to phase and amplitude for a signal at 1.575 GHz (GPS frequency) which is outside the theoretical limit of the modeling technique. A summary is provided of ray tracing simulations characterizing both phase and amplitude effects at frequencies from 3 to 17 GHz and axial positions from 0.25 m to 1.5 m. The results correlate well with known data. The low frequency measurements also provide good correlation to the trends exhibited in the simulations.

Nomenclature

A	Amplitude of the electric field (V/m)
c	Speed of light (3×10^8 m/s)
E	Electric field (V/m)
FN	Antenna pattern distribution function
k	Wave number (m^{-1})
k_{noise}	Wave number of plume oscillations
Isp	Specific impulse (s
m_{amp}, m_{freq}, m_{phase}, m_{noise}	Modulation Factors for amplitude (unitless), frequency (rad/s), phase (rad), and density noise or oscillations (unitless)
l_{Npl}, l_{Nnopl}	Length of ray tube with and with out a plasma present for ray N
N	Index of ray
n_e	Electron number density (m^{-3})
N_{max}	Number of rays
n_0 λ, n	Coefficients in static plume model
n_{stat}, n_{temp}	Static, temporal electron density models
Patt	Relative antenna power (to free space) (dB or W)
r	Radial distance from thruster.
s	Position of ray
t	Time (s)
w	Width of ray tube
x_{Npl}, x_{Nnopl}	Position of rays relative to center of antenna
$\Delta\phi_{RN}$	Phase shift of received wave relative to phase with out a plasma
ε_o	Free space permittivity (8.854×10^{-12} F/m)
ε_r	Relative permittivity
ϕ_{ant}	Phase shift of antenna (relative to free space) (rad)
$\phi(t)$	Phase of wave at time, t (rad)
ϕ_{nopl}	Phase of wave without a plasma
λ_0	Wavelength (m)
μ_0	Permeability of free space ($4\pi\times10^{-7}$ H/m)
σ	Standard deviation of Gaussian function (m)
θ	Angle from thruster center line
ω	Radial frequency (rad/sec)
ω_{noise}	Radial frequency of plume oscillations
ω_p	Radial plasma frequency

*Graduate Student Research Assistant, Electrical Engineering and Computer Science, member AIAA

†Graduate Student Research Assistant, Applied Physics Department

‡Assistant Professor, Electrical Engineering and Computer Science, member AIAA

§Assistant Professor, Aerospace Engineering, member AIAA

1•Introduction

Stationary plasma thrusters (SPT's) are currently being tested and considered for use aboard next generation spacecraft for North-South station keeping, repositioning, and orbit transfer due to their high thrust efficiency and nearly optimal specific impulse (I_{sp})[1]. The advantage of using an SPT in these

satellite missions is increased propellant utilization mass efficiency resulting in an increase in satellite lifetime and increased payload mass. However, consideration must be given to possible interactions with satellite electromagetic systems such as for communication, navigation, and remote-sensing since the thruster generates a dense plasma plume. Therefore, the effect of the SPT on satellite sub-systems must be established.

Electromagnetic signals are known to interact with a plasma [2-4] by altering the phase, amplitude, direction, and power spectral density of a transmitted signal such as described in Equation 1:

$$E = A\left[1 + m_{amp}(t)\right] \times \cos\left[\left(k(r)r - (\omega - m_{freq}(t))t - m_{phase}(t)\right)\right]. \quad (1)$$

The plume-signal interaction is determined by the electromagnetic dispersion relation, which is primarily dependent on electron number density and the gradients of electron number density (both are time varying in the SPT plume). The plume can impact an electromagnetic signal up to three different ways: amplitude, frequency, or phase. Amplitude and phase noise are produced by electron density oscillations in the SPT plume; however, the plume does not directly alter the frequency component. Modification of these basic parameters needs to be generally characterized both experimentally and through computer modeling in order to determine the effect on particular systems of interest where signal to noise degradation can significantly affect data rates or signal resolution.

Previous investigations of the SPT have partially characterized the impact to electromagnetic signals. These studies characterized the phase noise and power spectral density at a number of frequencies between 2.6 GHz and 17 GHz [5-7] and the amplitude attenuation due to beam spreading was measured at 17 GHz [7]. These measurements provide direct indication of the plume impact on phase, amplitude, and power spectral density which also provide validation of the computer simulations. The simulations using ray tracing are based on the electron number density [5, 7]where a temporal density model [5] has been introduced to simulate the phase oscillations produced by the thruster.

The previous experimental studies have characterized the plasma over a range of frequencies; however, no experiments have been completed where the transmission frequency is less than the peak plume plasma frequency along the transmission path which could potentially cause significant attenuation and added noise. Additionally, simulations have modeled the phase noise produced by the plume, but no modeling technique has been reported to estimate of the amplitude noise produced by the plume. A number of modeling and experimental issues are addressed in this paper. In particular, amplitude noise is modeled through simulation of time varying attenuation levels (where phase noise has been previously simulated [5]). Modeling this phenomena through ray tracing is possible through determination of the signal beam spreading (Section 2). Additionally, experimental efforts at low frequencies (1.5 GHz) are needed to characterize the effect on transmission parameters due to the significant impact at frequencies approaching the plasma frequency of the plume. At these lower frequencies (longer wavelengths), the ray tracing method decreases in accuracy since the wavelength is on the order of the density gradient scale length in the thruster plume. Experimental characterization of phase, amplitude, and power spectral density, therefore, provides baseline information for system analysis and simulation validation (Section 3). In this paper the low frequency measurements are compared to the ray tracing results of the lowest frequency simulation possible with ray tracing. To summarize the modeling and experimental results, the attenuation and oscillation levels are compared for a range of values for frequency and spatial position (Section 4).

2• Computer Simulation of Amplitude Modulation Using Ray Tracing

Ray tracing is an extremely useful tool for predicting high frequency electromagnetic transmission characteristics[8-10]. This section first reviews the ray tracing technique and suggests a source of amplitude modulation, then describes the physical simulation scenario, and finally, demonstrates amplitude modulation of a transmitted signal.

General Theory of Ray Tracing

Ray tracing separates the components of the electromagnetic fields so that the amplitude, phase, and path are traced individually. The attenuation and phase of the signal are predicted by integrating the wave number along the ray path. The attenuation is predicted through the imaginary part of the wave number which is negligible for the SPT-100 plume [7], and the phase is tracked (Equation 2) by using the real part of the wave number (Equation 3a).

$$\phi_2(s_2) - \phi_1(s_1) = \int_{s_1}^{s_2} k(\bar{r},t)\,ds \quad (2)$$

$$k(\bar{r},t) = \frac{\omega}{c}\sqrt{1 - \frac{\omega_p^2(\bar{r},t)}{\omega^2}} = \omega\sqrt{\mu_o \varepsilon_o \varepsilon_r(\bar{r},t)} \quad (3a)$$

$$\omega_p^2(\bar{r},t) = \frac{n_e(\bar{r},t)e^2}{\varepsilon_o m_e} \quad (3b)$$

The ray path follows the gradients of the electron density:

$$\frac{\partial}{\partial s}\left[\sqrt{\varepsilon_r(\bar{r},t)}\hat{s}\right] = \nabla\sqrt{\varepsilon_r(\bar{r},t)} \tag{4}$$

where the relative permittivity is related to the electron number density through Equations 3a and 3b.

Using ray tracing, the power density of an individual ray is found through the conservation of power. The total power in a single ray is constant since loss of power due to plasma heating is minimal [11]; therefore, reduction in power density is attributed to beam spreading. This is quantified by assuming that the power of an individual ray flows through a tube (called a ray tube as in Figure 1). The ray tube cross-sectional area varies proportionally with the degree of refraction. The reduction in power is proportional to the ratio of the area at a reference point (transmitter) to the area at an observation point (receiver):

$$S_{rec} = \frac{A_{trans}}{A_{rec}} S_{trans} \tag{5}$$

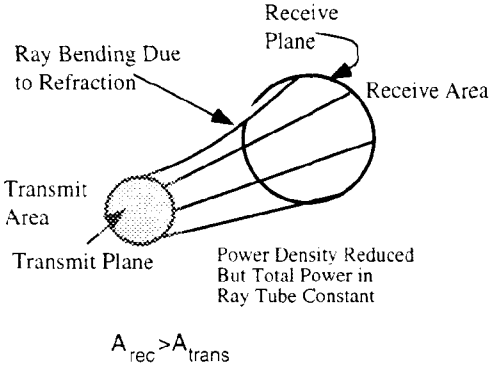

Figure 1. Ray Tube Analysis Produces the Change in Power Density

Using these basic equations and a temporal and spatial density model [5, 7], the phase change, ray path, and power density reduction (attenuation) are predicted for a wave traversing the plume of an SPT. The phase shift and noise have been experimentally measured [7] and also simulated using a temporal plume model [5]. The ray path divergence has been demonstrated through measurement of signal attenuation [7]. In this work, amplitude modulation due to variable attenuation is modeled through ray tracing simulations of a Ku-band antenna using a temporal plume model.

Physical Simulation Scenario

The ray tracing analysis is applied to transmission paths in a plane orthogonal to the flow of plasma, 0.15 m from the exit plane of the thruster, where the center of the antenna intersects the axis of the thruster (see Figure 2). This axial distance is chosen to provide comparison with previous measurements with Ku-band horn antennas operating at 17 GHz [7]. The computer model simulates the coupling between the two antennas through a standard Gaussian distribution,

$$FN = \frac{1}{\sqrt{2\pi\sigma}}\exp\left[-\frac{1}{2}\left(\frac{x}{\sigma}\right)^2\right] \tag{6}$$

with standard deviation of 0.024 m [11]. A square root of FN is taken to separate the effects of the transmit and receive antennas.

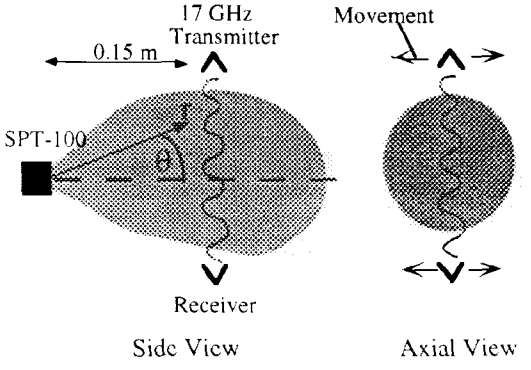

Figure 2. Physical System for Ray Trace Modeling.

The electron density is taken from measurements of an SPT-100 operating at nominal conditions of 300 V, 4.5 A, and 5.8 mg/s of xenon. The density model is the product of a static model and a temporal model. The static density is given by Equation 7 [7] where r and θ are shown in Figure 2 and the temporal model is given by Equation 8 [5]:

$$n_{stat}(r,\theta) = C_1\exp\left(-\left(\frac{r\sin\theta}{C_2}\right)^2\right) + \frac{C_3}{r^2}\exp\left(-\frac{\theta}{C_4}\right) \tag{7}$$

C_1=4.7x10^{16} m^{-3}, C_2=0.073 m,
C_3=1.3x10^{15} m^{-1}, C_4=1.1 rad.

$$n_{temp}(\bar{r},t) = 1 - m_{noise}\cos\left(\omega_{noise}t - k_{noise}\bar{r}\right) \tag{8}$$

m_{noise} = 0.12, ω_{noise} = 2πx6x10^3 rad/sec,
k_{noise}=10.9.

The density oscillation frequency is ideally represented as the entire frequency spectrum of the thruster; however, for simplicity in demonstration of the

amplitude modulation the dominant oscillation frequency (26 kHz) is used to represent the density oscillations. This assumption provides worst case results for noise produced by the plume.

Amplitude Modulation Simulations

Our ray tracing method utilizes a combined static and temporal model of the SPT plume. In the simulations, the rays bend (Figure 3) slightly producing small attenuation; however at lower frequencies the attenuation is more severe as shown later in Section 4. The attenuation due to the plasma is calculated for each ray tube by finding the change in area of the ray tube (see Figure 4). The initial or transmitted area is determined by the simulation parameters. The final or receiver ray tube area is determined by two dimensions: 1) the length between the rays in the simulation plane which is determined by the simulation and 2) the length in the direction orthogonal to the simulation plane which is assumed constant since the density gradient is much less in that direction, thus producing minimal refraction.

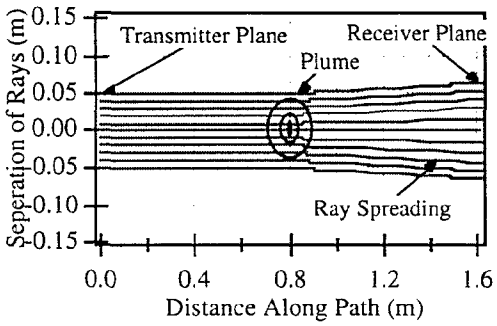

Figure 3. Ray Paths of the Simulated Antenna for a Single Time Step (0.15 m, 17 GHz).

A series of rays are used to simulate an antenna aperture through the superposition of the electric fields across the aperture. The amplitude and phase of each ray are used to find the field quantities which are then weighted by the antenna distribution function. The amplitude and phase of the individual rays are plotted in Figures 4 and 5. The amplitude of the rays actually has a power gain on the edge of the plume where the rays density is higher than in free space. The weighted fields are distributed across each ray tube so that the power density is constant across a ray tube. The sum of the weighted fields is used to find the total power at the receiver. The calculations are summarized in expressions for attenuation and phase (Equations 9a and 9b) for an antenna with a distribution function, *FN*.

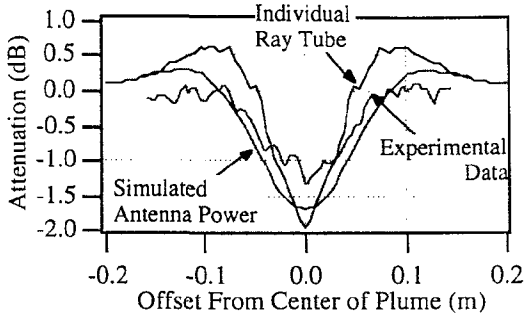

Figure 4. Power Change Due to Plasma for Individual Ray Tubes, Simulated Antenna, and Experimental Results; 0.15 m downstream, 17 GHz.

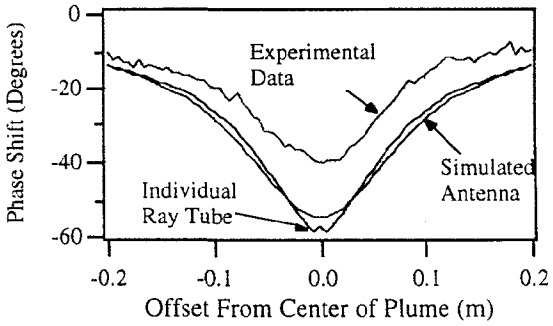

Figure 5. Phase Shift Due to Plasma for Ray Tubes, Simulated Antenna, and Experimental Results; 0.15 m downstream , 17 GHz.

$$P_{att} = \frac{\left| \sum_{N=1}^{N_{max}} \sqrt{wl_{Npl}} \left[FN(x_{Npl}) \right]^{1/2} \left[FN(x_{Nnopl}) \right]^{1/2} \left(\frac{l_{Nnopl}}{l_{Npl}} \right)^{1/2} e^{j\Delta\phi_{Npl}} e^{j\phi_{Nnopl}} \right|^2}{\left| \sum_{N=1}^{N_{max}} \sqrt{wl_{Nnopl}} \left[FN(x_{Nnopl}) \right] e^{j\phi_{Nnopl}} \right|^2} \tag{9a}$$

$$\phi_{ant} = angle\left\{ \sum_{N=1}^{N_{max}} \sqrt{wl_{Npl}} \left[FN(x_{Npl}) \right]^{1/4} \left(\frac{l_{Nnopl}}{l_{Npl}} \right)^{1/2} e^{j\Delta\phi_{Npl}} e^{j\phi_{Nnopl}} \right\} - angle\left\{ \sum_{N=1}^{N_{max}} \sqrt{wl_{Nnopl}} \left[FN(x_{Nnopl}) \right] e^{j\phi_{Nnopl}} \right\} \tag{9B}$$

The attenuation and phase for a simulated antenna are calculated from Equations 9a and 9b, and results are shown in Figures 4 and 5. The individual ray tube results exhibit slight noise which is attributed to the numerical aspects of ray sampling and step size. In both the attenuation and phase, the plots show the expected relationship between the individual rays and the antenna; the antenna results are the convolution of the individual rays and the antenna function.

In addition, experimental data are also plotted in Figures 4 and 5 for comparable conditions. For both amplitude and phase, the simulation tends to over predict the effect of the plume on the transmitted signal when compared to the experimental data (5% for attenuation and 30% for phase). These differences can be attributed to the inherent limitations of the ray tracing technique. Two simulation limitations are the finite ray sampling and step size both having greater importance at smaller wavelengths where the error tends to affect the phase more than the amplitude. Two other limitations are the electron density model which is known to be accurate only to ±20% and the limited accuracy of the antenna distribution function. Given these factors, the difference between the ray tracing simulations and the experimental measurements are expected.

When the attenuation level varies over time due to oscillations in density, then amplitude noise or modulation is produced on the transmitted signal (Figure 6). The most attenuation is -1.92 dB and least is -1.46 dB. The variation of ±0.23 corresponds to the experimental noise in Figure 4. The simulations have been implemented with a 26 kHz plasma oscillation which is the dominant frequency component; however, amplitude variation of smaller magnitude exists for other frequencies.

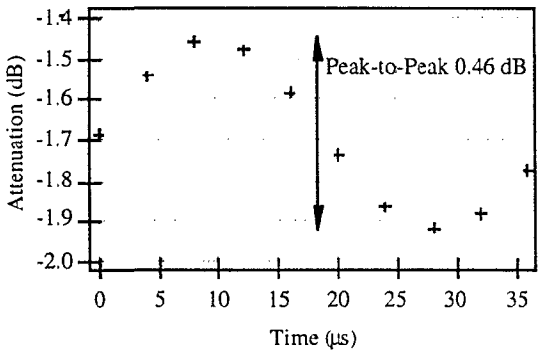

Figure 6. Simulated Amplitude Variation Over Time for a 17 GHz Signal Transmitted Through the Plume 0.15 m from the Exit Plane (Relative to Power With no Plume Present).

The ray tracing simulation indicates amplitude modulation at 26 kHz which is described mathematically by Equation 1. In that equation the modulation factor, m_{amp}, is represented by $|m_{amp}|\cos(\omega_{oscill}t)$ where ω_{oscill} is the radial frequency of the density oscillation and $|m_{amp}|$ is the peak-to-peak signal amplitude normalized by the mean amplitude value. $|m_{amp}|$ is found to be 0.053 (note: this is a unitless number, not dB) and the mean attenuation is -1.68 dB (0.68 V/m). The corresponding phase variation (Figure 7) is found through similar methods where m_{phase} is $|m_{phase}|\cos(\omega_{oscill}t)$. $|m_{phase}|$ is the phase variation in degrees relative to the mean phase value ($|m_{phase}| = 0.094\text{rad}(5.4°)$), The phase shift relative to transmission through a vacuum is -0.96 rad (-55°).

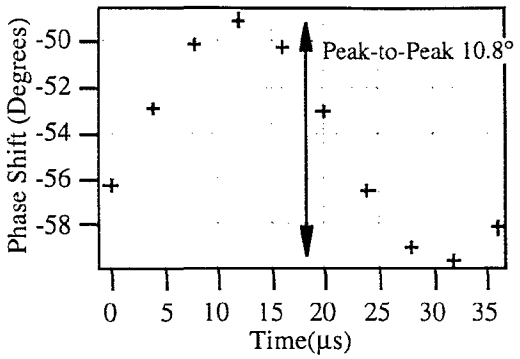

Figure 7. Simulated Phase Variation Over Time for a 17 GHz Signal Transmitted Through the Plume 0.15 m from the Exit Plane (Relative to Power With no Plume Present).

The power spectral density is a useful description for determining the quality of an electromagnetic signal. Ideally, the carrier power would be contained in a narrow bandwidth relative to the modulation and the noise power would be near the thermal noise floor (<<-100 dB) for a wide range of frequency offsets. The power spectral density is calculated for a 17 GHz signal transmitted through the plume 0.15 m from the exit plane using modulation parameters from the ray tracing simulation (Figure 8a).

The plasma oscillations produce 26 kHz harmonics where the first harmonic is produced through a combination of the amplitude and phase modulation. In this particular case, the amplitude modulation produces 3 dB more power in the first harmonic than with the phase modulation alone. The first harmonic compares well (within 2 dB) with the measured results in Figure 8b; however, the simulation under predicts the measured second harmonic. In addition, the broad band noise exhibited in the measurements are not predicted by the single

frequency oscillation model. These similarities and differences are common throughout other comparisons of the simulations and experiment. The differences between simulations and experiments would decrease with a more accurate model of the frequency spectrum of plume oscillations.

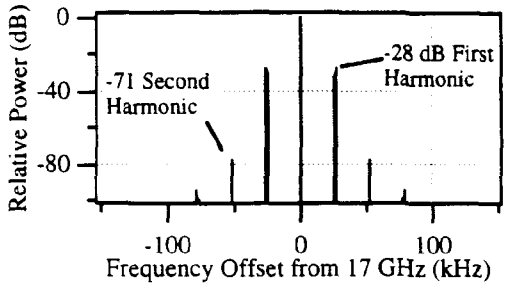

(8a) Simulated Effect of Density Oscillations

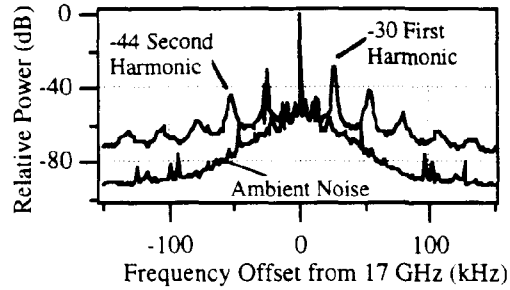

(8b) Measured Power Spectral Density

Figure 8. Comparison of the Measured and Simulated Power Spectral Density of a 17 GHz Signal Transmitted Across the Plume 0.15 m from the Exit Plane.

In summary, density oscillations in the plume produce both amplitude and phase modulation. This evaluation demonstrated the mechanism of amplitude modulation by the plume through ray tracing simulations. Additionally, the simulations compared well to phase, amplitude, and power spectral density measurements for a similar experimental situation.

3• Signal Characterization at 1.575 GHz

Experimental characterization at 1.575 GHz is important because ray tracing simulations at this frequency are not possible. In this section, initially the experimental system is overviewed, then the baseline noise levels are reported, the potential chamber impact is addressed, and finally the results are summarized and assessed.

Experimental Setup

An L-band (1.12-1.7 GHz) microwave measurement system (Figures 9 and 10) has been employed to measure the attenuation, phase shift, spectral power distribution, and phase noise of a 1.575 GHz signal (GPS frequency) through the xenon plasma exhaust of an SPT-100 thruster. This system consists of two Yagi-Uda antenna arrays, microwave coaxial cable, a microwave isolator, an amplifier, support structure, a computerized positioning table, and a computer controlled network analyzer and spectrum analyzer. With the exception of a some baseline experiments, all measurements have been performed at the Plasmadynamics and Electric Propulsion Laboratory (PEPL) at the University of Michigan in a 9-m x 6-m diameter stainless steel vacuum chamber ([12] for more information concerning PEPL).

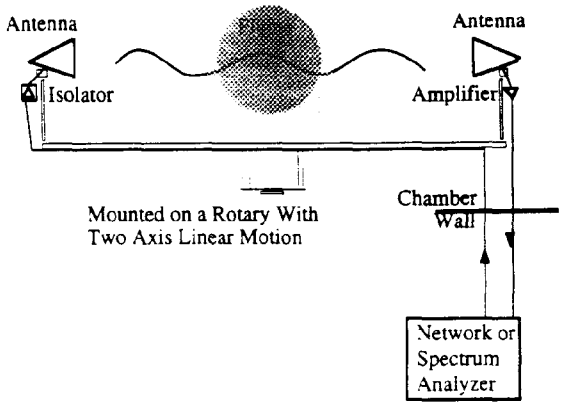

Figure 9. Side view of L-band Antenna Experiment.

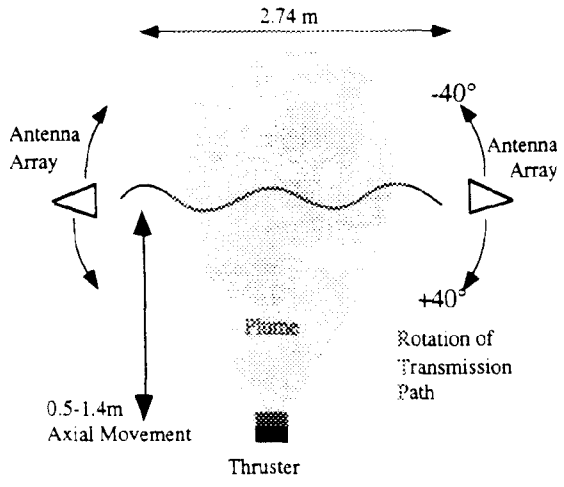

Figure 10. Top View of L-band Antenna Experiment.

All components except the network analyzer, spectrum analyzer, and computers are placed in the vacuum chamber. The assembled microwave system (illustrated in Figure 9) mounts onto the positioning table which has one rotational and two translational degrees of freedom. These types of motion make it possible to measure the transmission parameters of the microwave signal at several positions along the thruster's axis and also at several azimuthal positions relative to the thruster's centerline.

The microwave measurement system developed for this experiment was designed to operate within the L-band (1.2 - 1.7GHz), though the GPS frequency was isolated in the data analysis. The two 13-element Yagi antennas have a bandwidths of 80 MHz with a center frequency of 1.575 GHz, gain of 12 dB, and a half power beamwidth of 40°. Mounted on the 3.3 m support structure tip-to-tip separation is 2.74 m.. Given the breadth of this structure and the width of the chamber with the metal panels, the rear of the antennas were on average a distance of 0.79-m from the chamber walls. This measurement system applied the capabilities of our network analyzer as a highly sensitive microwave transmitter and receiver. In particular, the narrow receiver bandwidth (<1kHz) of the network analyzer is extremely useful for measurements in noisy environments such as the SPT plume. In addition to the extremely stable phase and amplitude produced by the network analyzer which are important for differential measurements, the time gating feature of the network analyzer is utilized to isolate the received signal from the various reflections at the chamber walls. In order to further improve the signal response, an isolator and amplifier are added to the microwave system as in Figure 9. The microwave isolator (20 dB isolation) is inserted in the electrical path between the source or oscillator (the network analyzer) and the transmitter antenna to reduce reflections in the transmission line. The amplifier (30 dB) is inserted into the electrical path between the receiving antenna and the network analyzer to compensate for coaxial cable and free space transmission loss.

The noise characteristics of the microwave system have been assessed with and with out the plasma present. The measurement uncertainty is summarized by short term measurement variation and long term drift where the drift can systematically be removed from the measurement when necessary. In transmission experiments with out the plasma, the variation in amplitude and phase is found to be ±0.01 dB and ±0.01° respectively. The same noise values increased with the plasma present are ±0.1 dB and ±1° which indicates significant noise coupling from the plasma plume. The measurement drift is estimated to be less than 0.5 dB and 2° over the course of a 24 hour period.

The characteristics of microwave propagation can potentially be distorted when propagation occurs in a metal cavity such as a vacuum chamber. The chamber resonance effect is especially pronounced when the wavelength is on the order of the chamber dimensions. In the PEPL chamber, the wave at 1.575 GHz (0.19 m wavelength) is 3-4% of the chamber size which is small but potentially still significant. In order to assess the potential chamber effects, comparable baseline experiments have been completed in both the vacuum chamber and open air configurations. The test results indicate small but measurable differences when characterizing transmission parameters inside the PEPL vacuum chamber. The parameter variation is estimated to be with 0.5 dB for amplitude and 2° for phase.

Experimental Results

The microwave transmission parameters have been characterized for a commercial grade stationary plasma thruster (Figure 11) built by the Russian Fakel Enterprises, and is presently on loan from Space System/Loral. The thruster has been previously tested at NASA Lewis [1, 5, 13-17]. The SPT-100 was nominally operated at 300 V and 4.5 A for the discharge and used xenon propellant flowing at 5.8 mg/s total (0.29 mg/s to the cathode). The tank pressure for the experiments was maintained below $7x10^{-4}$ Pa ($5x10^{-5}$ Torr) throughout the experiments.

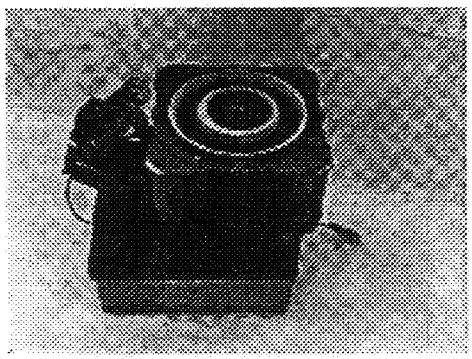

Figure 11. Stationary Plasma Thruster, SPT-100

The degrees of freedom offered by the positioning system allowed measurements to be taken for a range of centerline positions, with an added ability of measuring the signal for a range of azimuthal positions at each axial location. In this experiment, we measure the attenuation, phase shift, and power spectral density of the signal at 0.508, 0.610, 0.711, 0.813, 0.914, 1.016, 1.219, 1.321, and 1.422 m from the exit plane of the thruster, with angular positions set to 0°, 10°, 20°, 30°, and 40° relative to the position shown in Figure 10.

The attenuation and phase characterization (see Figures 12 and 13) indicate a number of general trends for variation of the measurement positions. Due to the propagation path difference the amplitude and phase vary for different azimuthal positions with the phase more sensitive to position than the amplitude. This variation is well within the accuracy of the measurements, but is small relative to the necessary accuracy for system impact evaluation; therefore, in the ray tracing simulations, information from simulations where the propagation path is orthogonal to the thruster axis can be applied to more realistic off angle configurations. The attenuation, as expected, increases for decreasing axial position where the closest measurement point finds an attenuation between -18 and -26 dB. Additionally, the measurements show significant power loss even at the farthest measurement position (1.4 m). The phase shows greater sensitivity to density variation, but the general trends in phase are consistent throughout the testing region. Significant phase shifts (>360°) have been measured which could potentially impact phase sensitive systems.

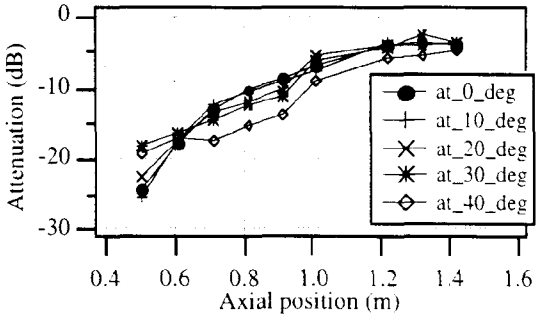

Figure 12. Attenuation Levels for 1.6 GHz Transmission Across the Plume for Various Axial Positions and Transmission Angles.

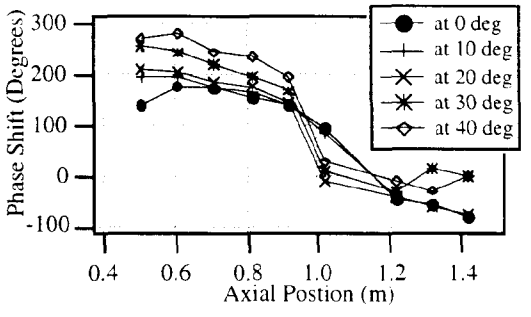

Figure 13. Phase Shift for 1.6 GHz Transmission Across the Plume for Various Axial Positions and Transmission Angles.

Power spectral density information has been obtained over the same position set as the amplitude and phase. A representative measurement is contrasted to measurements at 17 GHz and a baseline ambient measurement (Figure 14). As expected the lower frequency couples into the plasma much more strongly than the 17 GHz signal. The 1.575 GHz signal has as much as 30 dB more noise power than the 17 GHz system and as much as 40 dB higher than the noise floor of the microwave system without the plasma present. As with the 17 GHz system, the most significant coupling occurs at the dominant plasma oscillation frequency, 26 kHz. At the closest measurement point (0.5 m), the added noise is only 15 dB below the primary signal and even at the farthest measurement (1.4 m) the 26 kHz is still within 40 dB of the primary signal. Additionally, the trend in the power spectral density is towards higher levels of noise relative to the main signal for smaller axial distances. This trend is primarily driven by the decrease in received power as opposed to increased noise coupling. In general, the noise power induced by the plume is much higher than the system noise power without the plume present and could potentially degrade electromagnetic link characteristics.

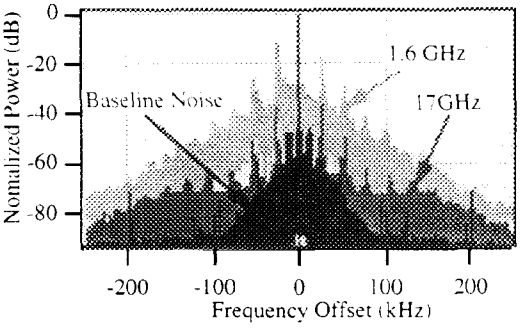

Figure 14. Comparison of Power Spectral Density of Signal Transmitted at 0.5m for 1.6 GHz, 17 GHz, and a Common Baseline without a Plume

4• Discussion

The SPT plume affects the phase, amplitude, and power spectral density of a transmitted electromagnetic signal. The signal impact is evaluated over a wide range over frequencies and transmission paths using the ray tracing algorithm. The 1.575 GHz measurements are below the simulation capabilities of ray tracing, but the trends in the simulations are compared to the low frequency measurements. Finally, the theoretical limitation of ray tracing is suggested as a boundary for significant power loss.

The ray tracing technique is used to establish trends in the impact of both amplitude and phase to a transmitted signal. These simulations are completed for 0.25, 0.5, 1, and 1.5 m from the thruster exit

plane and for transmitted signals of 3, 4, 5, 6, 7, 9, 12, 15, and 17 GHz. The static density model uses Equation 7 for the 0.25-m and 0.5-m cases, Equation 10 [Dickens]

$$n_{static}(r,\theta) = \frac{n_o \exp\left\{-\left[\lambda(1-\cos\theta)\right]^n\right\}}{r^2 \cos^2\theta} \qquad (10)$$

$$n_0 = 10^{16}\ m^{-1},\ \lambda = 50,\ n = 0.6$$

for 1.5-m case, and the mean density of the two models for 1-m case. The temporal model follows Equation 8. All of the summary simulations are calculated for the plume effect on a single ray in order to make the results more general. This implementation produces worst case results for transmission across the plume since the center ray experiences the greatest impact.

The attenuation simulations are completed for a wide range of situations (Figures 15 and 16). The attenuation indicates a sharp increase in power loss at the lower frequencies, but also a quick reduction in plume impact with increasing distance. The results show less than 3 dB attenuation for frequencies greater than 10 GHz except for the very closest positions. The modulation coefficient follows similar trends indicating up to 25% modulation at the closest measurement point at 3 GHz and also indicating less than 5% modulation for all distances at 17 GHz; however, as was demonstrated earlier with the 17 GHz simulation, even small modulation coefficients produce significant increases in the noise power.

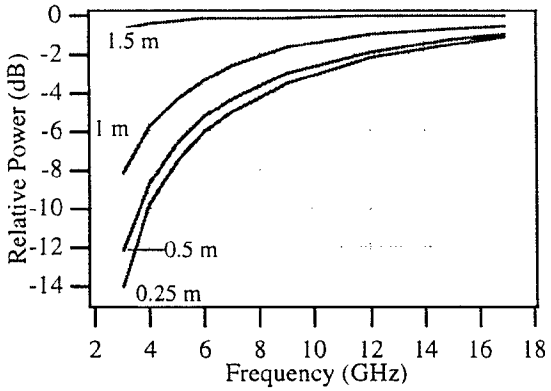

Figure 15. Simulated Attenuation of an Electromagnetic Signal Transmitted Through an SPT Plume

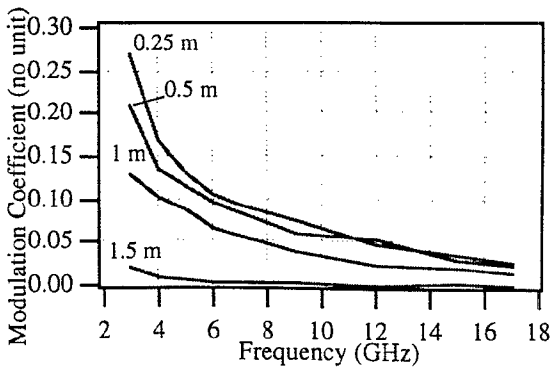

Figure 16. Simulated Amplitude Modulation Coefficient of an Electromagnetic Signal Transmitted Through an SPT Plume

The phase simulations are completed over the same spatial and frequency simulations set as the attenuation (Figures 17 and 18). The phase is more sensitive to simulation error than the amplitude as the frequency approaches the theoretical limit of geometrical optics; hence, the lower frequency values at the closest simulation point did not produce reliable results. Overall, the general trends are similar to the attenuation simulations; however, the rate of decline in the signal impact is slower as the frequency or position increases. Again, even a small modulation factor can produce significant increase in the noise power.

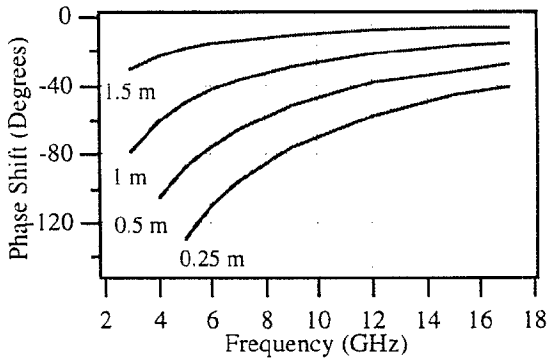

Figure 17. Simulated Phase Shift of an Electromagnetic Signal Transmitted Through an SPT Plume (Referenced to the Phase Shift with no Plasma).

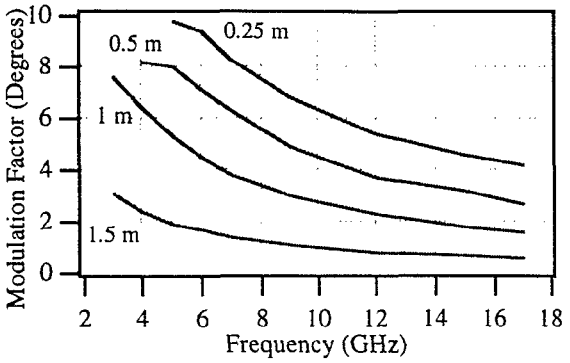

Figure 18. Simulated Phase Modulation Factor of an Electromagnetic Signal Transmitted Through an SPT Plume.

The experimental measurements at 1.575 GHz produced a number of facts useful for understanding the limitations and implications of the ray tracing simulation. First, the independence of attenuation and transmission angle with respect to the thruster axis provides flexibility to use the amplitude simulations for any path crossing a similar axial position. Second, the data from Figures 12 and 13 that corresponds to Figures 15 and 17 follows the trends of the simulation curves despite the failure of the simulation at this frequency. Third, the power spectral density indicates significant modulation by the plasma as would be implied by the trends in Figures 16 and 18 and the lower frequencies.

The theoretical limit of geometrical optics, Equation 11 [10], states the wavelength must be much smaller than scale length of changes in the wave number or in this case the permittivity (which directly relates to the density).

$$\lambda_o << \frac{\varepsilon_r}{\frac{\partial}{\partial path}\varepsilon_r} \qquad (11)$$

This condition implies that if the density changes quickly, the ray will bend faster than ray tracing can reliably predict. In some instances, the plasma appears to be a perfect conductor under the circumstances where this condition fails.

The condition for validity of the ray tracing analysis is evaluated for a geometry similar to Figure 2 for a range of axial positions. For any given position the failure point for the highest frequency is along the thruster axis. The contour defining the limiting frequency is plotted in Figure 19. Using this condition as a boundary, the attenuation below the limit is expected to be greater than 10 dB and potentially much worse than 10 dB. This conclusion is drawn from the experimental results at 1.575 GHz and extrapolation of the ray tracing simulations.

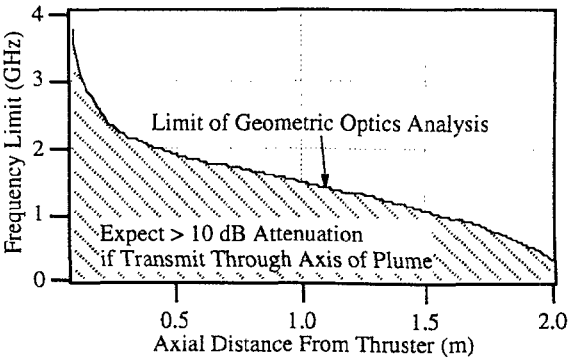

Figure 19. Theoretical Frequency Limit of Geometric Optics With Respect to Transmitting Across the Plume at a Given Axial Distance From the Thruster Exit Plane.

Acknowledgments

This research was funded in part by AFOSR grant #F49620-95-1-0331 (contract monitor: Dr. M. Birkan). The authors would like to thank several of the students at PEPL including S.W. Kim, J. Haas, M. Domonkos, C. Marrese, J. Foster, and L. King whose help made the experiments happen. Thanks also goes to J. Mahowal for assistance with the low frequency experiments, C. Nelson for his work on the ray tracing simulations, and S. Bilen for his assistance with the final paper and presentation. We also wish to thank M. Day from Space Systems/Loral for the loan of the SPT-100.

Bibliography

1. Myers, R.M. and Manzella, D.H., *Stationary Plasma Thruster Plume Characteristics*, IEPC-93-096, in *23rd International Electric, Propulsion Conference*, Seatle, WA, 1993.
2. Heald, C.B. and Wharton, M.A., *Plasma Diagnostics With Microwaves*, New York: John Wiley and Sons, Inc., 1965.
3. Sheffield, J., *Plasma Scattering of Electromagnetic Radiation*, New York, Academic Press, Inc., 1975.
4. Stix, T.H., *Waves in Plasmas*, New York, American Institute of Physics, 1992.
5. Dickens, J.C., Kristiansen, M., and O'Hair, E, *Plume Model of Hall Effect Plasma Thrusters with Temporal Consideration*. in IEPC 95-171. 1995, in *25rd International Electric, Propulsion Conference*, Moscow, Russia, 1995.

6. Dickens, J., *et al. Impact of Hall Thrusters on Communication System Phase Noise*. in *31st AIAA/ASME/SAE/ASEE Joint Propulsion Conference and Exhibit*, AIAA 95-2929, San Diego, CA, 1995.
7. Ohler, S., B. Gilchrist, and A. Gallimore. *Microwave Plume Measurements of an SPT-100 Using Xenon and a Laboratory Model SPT Using Krypton.*, AIAA 95-2931, in *31st AIAA/ASME/SAE/ASEE Joint Propulsion Conference*, San Diego, CA, July, 1995.
8. Ling, H., *et al.*, *Effect of an Arcjet Plume on Satellite Reflector Performance*, IEEE Transaction on Antennas and Propagation, **39**(9), p. 1412-1419, 1991.
9. Kim, H. and Ling, H., *High Frequency Electromagnetic Scattering From an Inhomogeneous Dielectric Body By Ray Tracing*. in *IEEE Antennas and Propagation Society Symposium*, Ontario, Canada, 1991.
10. Born, M. and Wolf, E., *Principles of Optics*, New York. Pergamon Press Book, 1964.
11. Ohler, S.G., Gilchrist, B.E., and Gallimore, A.D., *Non-intrusive electron number density measurements in the plume of a 1 KW arcjet using a modern microwave interferometer.* IEEE Transactions on Plasma Science, **23**(3), p. 428-435, June, 1995.
12. Gallimore, A., Reichenbacher, M., and Guiczinski, F., *Near and Far-Field Plume Studies of a 1kW Arcjet*, AIAA-94-3137 in *30th AIAA/ASMA/SAE/ASEE Joint Propulsion Conference*, Indianapolis, IN, June, 1994.
13. Absalamov, S.K., *et al. Measurement of Plasma Parameters in the Stationary Plasma Thruster (SPT-100) Plume and its Effect on Spacecraft Components*, AIAA-92-3156 in *28th Joint Propulsion Conference*, Nashville, TN, 1992.
14. Manzella, D.H. *Stationary plasma thruster plume emissions*, IEPC-93-097 in *23rd International Electric Propulsion Conference*, Seattle, WA, 1993.
15. Manzella, D.H. *Stationary Plasma Thruster Ion Velocity Distribution*, AIAA-94-3141 in *30th AIAA/ASME/SAE/ASEE Joint Propulsion Conference*, Indianapolis, IN, 1994.
16. Manzella, D. and Sankovic, J., *Hall Thruster Ion Beam Characterization*, AIAA 95-2927 in *31st AIAA/ASME/ASEE Joint Propulsion Conference and Exhibit*, San Diego, CA, July, 1995.
17. Dickens, J., *Communication Impact of Hall Effect Plasma Thrusters*, Doctoral Thesis, Texas Tech University, 1995.